



CBPF

CENTRO BRASILEIRO DE PESQUISAS FÍSICAS

Notas de Física

CBPF-~~10~~-006/83

LIFETIME EXPERIMENTS OF CHARMED PARTICLES

by

GERHARD OTTER

RIO DE JANEIRO

1983

Lifetime experiments of charmed particles

1. INTRODUCTION

In this report the present state of knowledge of the lifetime of charmed particles is summarized. It is not intended to treat the theoretical side of this problem, but the various experiments measuring charm lifetime will be discussed in detail. Since this lifetime is very short ($10^{-12} - 10^{-13}$ sec) experimental difficulties arise in finding and measuring the production and decay point of these particles as well as in measuring all of its decay products. We therefore need a vertex detector with very good spatial resolution and a connecting spectrometer for momentum measurement of the charged and neutral particles. To obtain unique results good particle identification of the investigated particles is further desirable. The experiments carried out up to now use emulsions, a special bubble chamber or an electronic device as vertex detector together with a suitable downstream spectrometer [1]. Details and results of these investigations will be discussed in this report.

Let us start with a very short introduction to charmed particle physics. We shall treat the quark content of charmed particles, as well as their decay properties. A number of review articles consider these items in much more detail [2].

Hadron spectroscopy and its regularities lead to the concept of subatomic particles, the quarks. Mesons are built up by a quark and an antiquark and baryons by three quarks. In the early days 3 kinds of quarks (u, d, s) were enough to describe the experimental data. With the detection of J/ψ [3] it became clear that a fourth quark (charmed quark c) exists and the corresponding symmetry is $SU(4)$. The quantum numbers of the 4 quarks are given in Table 1.

Table 1

	B	I	Q	S	Y	C
u	1/3	1/2	2/3	0	1/3	0
d	1/3		-1/3	0	1/3	0
s	1/3	0	-1/3	-1	-2/3	0
c	1/3	0	2/3	0	0	1

(B = baryon number, I = isospin, Q = charge, S = strangeness, Y = hypercharge, C = Charm).

The lowest-lying hadrons, i.e. the $J^P = 0^-$ -mesons ($q\bar{q}$: $4 \times 4 = 15 + 1$) and $J^P = 1/2^+$ -baryons (qqq : $4 \times 4 \times 4 = 4 + 20 + 20' + 20$, where the $1/2^+$ -states are realized by the $20'$ -multiplet) are displayed in fig. 1.

All charmed O^- -mesons are well known with the possible exception of the F^- [4], where recently doubts about the published mass were raised by finding the F^- -mass at a different value [5]. The $1/2^+$ -charmed baryons are less well known. Only $\Lambda_c^+ (\cong C_1)$ and $\Sigma_c^+ (\cong C_1)$ are definitively established and there are indications for the existence of the Λ [6].

From these charmed particles we report results on the lifetime of the weak decaying states D^+ , D^0 , F^+ and Λ_c^+ . Some important properties of these particles are given in table 2.

Table 2

	mass (MeV)	Spin-parity	S	I	quark decomposition
D^+	1869.4 ± 0.6	0^-	0	1/2	$c \bar{d}$
D^0	1864.7 ± 0.6	0^-	0	1/2	$c \bar{u}$
F^+	2021 ± 15	0^-	1	0	$c \bar{s}$
Λ_c^+	2282.2 ± 3.1	$1/2^+$	0	0	$c d u$

In 1970 a new model for weak interactions was proposed which turned out to be very successful [7]. In this GIM-model the charm quark c was introduced to explain the experimental smallness of the strangeness-changing weak neutral current. The weak charged current in the GIM-model is

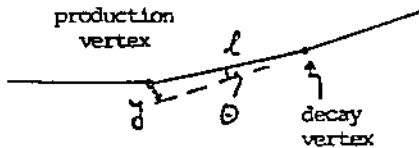
$$J_\mu = (\bar{u} \bar{c}) \gamma_\mu (1-\gamma_5) M \begin{pmatrix} d \\ s \end{pmatrix} \\ = (\bar{u} \bar{c}) \gamma_\mu (1-\gamma_5) \begin{pmatrix} d \cdot \cos \theta_c + s \cdot \sin \theta_c \\ -d \cdot \sin \theta_c + s \cdot \cos \theta_c \end{pmatrix}$$

with the Cabibbo angle θ_c . From the value of the Cabibbo angle ($\cos \theta_c = 0.97$ and $\sin \theta_c = 0.23$) we infer that the c -quark decays preferentially to the s -quark ($C \rightarrow S$ is Cabibbo allowed) and that the decay $c \rightarrow d$ is suppressed ($c \rightarrow d$ is Cabibbo forbidden). This result is qualitatively not changed when instead of the GIM-model with 4 quarks a 6-quark-model (the matrix M is then the Kobayashi-Maskawa matrix) is used [8].

Assuming that in first approximation only the Cabibbo allowed decays are important, the diagrams of fig. 2 are responsible for the weak decay of the charmed particles. The diagrams of the first row are those of the spectator model, where the c -quark decays and does not influence the other quarks (spectator quarks). A consequence of this spectator model is that the lifetime is the same for all 4 charmed particles. Other diagrams, however, could also be important for the weak decay of the charmed particles. These are W -exchange and annihilation diagrams as shown in the second row of fig. 2. For a pseudoscalar particle decaying into two light fermions their contribution seems to be small. The effect of helicity suppression, however, is irrelevant when gluons are exchanged as indicated in the figure. A consequence of the contribution of these non-spectator diagrams is a longer lifetime of the D^+ as compared to those of the other particles. All four charmed particles could have different lifetimes.

2. BUBBLE CHAMBER EXPERIMENTS

In a high energy reaction where charmed particles as well as other particles are produced, the charm decay can only be detected when at least one of the decay particles has an impact parameter y with respect to the production vertex which is larger than the experimental resolution in this experiment (see the drawing on this page). A spatial resolution in the order of 10 to 100 μm is therefore needed if we do not want to lose too many charm decays.



$$y = l \sin \theta = \frac{P_{\perp}}{P_{\parallel} + E} \cdot c \tau$$

P_{\perp} , P_{\parallel} , E transverse and longitudinal momentum, and energy of the decay particle, defined in the charmed particle rest system
 τ lifetime of the charmed particle.

Bubble chambers specially designed and built for the detection of charmed particles can achieve the required condition: their bubbles have small diameters ($< 50 \mu\text{m}$) and are produced with high density (> 70 bubbles/cm). Since bubbles in bubble chamber grow after they are formed the condition of small bubble diameter is achieved by decreasing the time between bubble production by the passing charged particle and photographing. For a normal bubble chamber as BEBC this flash delay is ~ 10 msec after which bubbles reach a diameter of $\sim 500 \mu\text{m}$. The specially built LEBC-bubble chamber works with ~ 300 usec flash delay and with bubbles of $\sim 40 \mu\text{m}$ diameter. When a higher temperature as normal is used as working point for the bubble chamber, the bubble density increases. LEBC produces ~ 70 bubbles/cm compared to a density of a factor of 10 smaller for normal bubble chambers.

Two methods have been used for the registration of these small bubbles. The first uses a special high resolution camera in combination with the bubble chamber. A great disadvantage is, however, that for this case the depth of field is limited, to a few millimeters where bubbles are sharply seen. The second possibility is to record these small bubbles with holographic techniques. This not only gives access to better spatial resolution, it also introduces the possibility of working with larger beam intensities. On the other hand holographic techniques are complicated and the reconstruction of tracks is not simple.

A) Experiment NA 16 [11]

This experiment, carried out at CERN, used the hydrogen bubble chamber LEBC (an acronym for LEXan Bubble Chamber) and the downstream spectrometer EHS (European Hybrid Spectrometer). The incident beams were a \bar{p} - and a p-beam at 360 GeV/c. A schematic layout of the experiment is given in fig. 3.

LEBC is a rapid cycling (30 Hz) cylindrical chamber of 20 cm diameter with a depth of 4 cm. Classical high resolution optics was used for the registration of the small bubbles of 40, μm diameter.

The downstream spectrometer EHS was equipped with large drift chambers (D1 - D5) for the reconstruction of the charged particle tracks. Since LEBC could not operate in a magnetic field, the large vertex magnet foreseen for the normal operation of EHS (shown in the fig. 3 as M1) was replaced by a 1.5 Tm magnet (M1') downstream of LEBC. This magnet and a second magnet (M2) serve for the momentum analysis of charged particles. EHS also provides gamma detection and reconstruction for nearly all π^0 's produced in the forward hemisphere (with an energy resolution of 1 - 3% for fully reconstructed π^0 's) using the detectors IGD and FGD. Furthermore a large volume drift chamber ISIS is used for ionisation sampling to identify charged pions in the 3 to 30 GeV/c momentum range.

In the meantime, the EHS has been improved by adding two Cerenkov counters, a transition radiation detector and a larger version of ISIS. The new experiment, called NA27, is still under analysis, results are not yet available.

For NA16, a total of 350 K pictures with incident π^- 's and 500 K pictures with incident protons have been taken. All films have been scanned twice and checked by physicists. Charm candidates in the bubble chamber have been detected by either searching for secondary tracks not pointing to the interaction vertex or by looking for increases of ionization. A scanning efficiency of 96% with no noticeable flight length dependence of the charmed particles down to ~ 1 mm has been inferred from the two scans. The bubble chamber measurements have been combined with the spectrometer information to obtain the momenta of the charged particles as well as of the reconstructed π^0 's. Kinematic fits have been carried out for the events and the much more abundant strange particle decays have been removed. The 52 charm decays having 2C or 3C kinematic fits are given in table 3. In case of ambiguity between Cabibbo-allowed and Cabibbo-suppressed interpretations, Cabibbo-allowed fits have been preferred. Moreover, Cabibbo-allowed D^{\pm} -hypotheses have been selected over any ambiguous A_c^+ or F^{\pm} -interpretation.

Table 3

	n = 0	= 1	= 2
D^0, \bar{D}^0			
$K^+ \pi^- \pi^0$	5	4	3
$K^+ \pi^+ \pi^- \pi^0$	8	2	0
$\pi^+ \pi^- \pi^0$	1	0	0
D^+, D^-			
$\pi^+ K^0 \pi^0$	0	2	0
$K^+ \pi^+ \pi^0$	13	4	1
$\pi^+ \pi^- \pi^0$	1	0	0
$K^0 \pi^+ \pi^- \pi^0$	1	0	0
F^{\pm}			
$K^+ K^- \pi^0$	0	3	0
D^+ / A_c ambiguous	1	0	0
F^+ / A_c ambiguous	2	0	1

Table 4

		n=0	n=1
D^0, \bar{D}^0	$K^{\pm} \bar{\nu} \pi^0$	1	0
	$K^{\pm} \bar{\nu} \pi^+ \pi^- \pi^0$	4	2
	$K^0 \pi^+ \pi^- \pi^0$	1	0
D^+, D^-	$K^{\pm} \pi^{\pm} \pi^0$	8	2
	$K^0 \pi^+ \pi^-$	1	0

Because of the relatively low beam energy, good limits on the momentum of the charmed particle (used for flighttime determination) can be obtained, despite the lack of complete neutral particle detection. 21 D^{\pm} and 22 D^0 -decays have been used to calculate the lifetime by maximum likelihood methods. The result of this investigation is the following:

$$21 D^{\pm} \quad \tau = (7.4^{+2.3}_{-2.0}) \cdot 10^{-12} \text{ sec}$$

$$22 D^0 \quad \tau = (6.8^{+2.3}_{-1.8}) \cdot 10^{-12} \text{ sec}$$

$$\tau_{D^{\pm}}/\tau_{D^0} = 1.1^{+0.6}_{-0.3}$$

C) Experiment NA18 [13]

This experiment has a much simpler experimental set-up than that of the other experiments discussed (see fig. 5). It consists essentially of two detectors only, a bubble chamber and a streamer chamber. The heavy liquid bubble chamber BIBC (acronym for Berne Infinitesimal Bubble Chamber) filled with freon C_2F_6 was used as vertex detector to recognize particles decaying near the interaction vertex. It worked in the high resolution mode with bubbles of 30 μm diameter and with a bubble density of 300 bubbles/cm. The 2m-streamer chamber filled with He-Ne-mixture at atmospheric pressure together with a 1.5 T magnet served to determine the momenta of the charged particles coming from BIBC. The apparatus could neither detect π^0 's nor identify charged relativistic particles by ionisation.

In a run with a ν^- -beam of 340 GeV/c, 155 K pictures with 95 K interactions were taken. The bubble chamber pictures were scanned for charm candidates within a projected forward cone of 20° and with decay lengths smaller than 25 mm. Since neutral particles could not be detected in this experiment, only candidates with no obvious missing neutral and with all tracks pointing into the streamer chamber were reconstructed geometrically using both the BIBC and the streamer chamber track information. From this sample 456 events were found where all tracks matched between the two detectors. Assigning to the tracks mass values according to Cabibbo-allowed charm decays and calculating the corresponding invariant mass of the charm candidate, 9 D^0 , 7 D^{\pm} and 5 F^{\pm} decays remained with masses in the interval of 1820 - 1910 MeV for D and 1960 - 2110 for F resp. and with decay lengths larger than a minimum value. Out of the 7 D^{\pm} candidates 4 fitted an F-mass with comparable probability. The F-decays were only accepted when they were not ambiguous to D-decays. The following events were found (Table 5)

-7-

Table 5

D^0, D^0	$K^+ \bar{\pi}^+$	3
	$K^+ \bar{\pi}^+ \pi^-$	6
D^\pm	$K^\pm \bar{\pi}^\pm \pi^\pm$	6
	$K^\pm \bar{\pi}^\pm \pi^\pm \pi^\mp$	1
F^\pm	$K^+ K^- \bar{\pi}^+$	2
	$\pi^\pm \pi^\pm \pi^-$	2
	$\pi^\pm \pi^\pm \pi^\mp \pi^\mp$	1

The lifetimes of these charmed particles were determined by the maximum likelihood method. The results are:

$$9 D^0: \quad \tau = (1.4 \begin{smallmatrix} + 2.6 \\ - 1.3 \end{smallmatrix} \pm 0.5) \cdot 10^{-13} \text{ sec}$$

$$7 D^\pm: \quad \tau = (6.3 \begin{smallmatrix} + 4.8 \\ - 2.3 \end{smallmatrix} \pm 1.5) \cdot 10^{-13} \text{ sec}$$

$$5 F^\pm: \quad \tau = (4.4 \begin{smallmatrix} + 5.0 \\ - 1.7 \end{smallmatrix} \pm 1.5) \cdot 10^{-13} \text{ sec}^*)$$

$$\tau(D^\pm)/\tau(D^0) = 1.5 \pm 1.0$$

*) this value is not reported in the publication, it was found in a conference report [13].

3. EMULSION EXPERIMENTS

Among the experiments designed for lifetime measurement, those with an emulsion as vertex detector together with a downstream spectrometer can be used even for lifetimes below 10^{-13} sec, due to the especially good spatial resolution of $\sim 1 \mu\text{m}$ in the emulsion, which is much better than in other detectors. There are, however, disadvantages when emulsion-vertex-detectors are applied: it is extremely difficult and time consuming to scan and measure the vertex of an interaction and the connecting particle tracks. As the emulsion is continuously sensitive and no timing information is possible, every charged particle passing through the emulsion is recorded, producing a large background. For charm production in the emulsion, neutrino beams are therefore best suited because $\sim 10\%$ of all neutrino interactions at high energy lead to charmed particle production. Emulsion experiments with photon beams were also performed, although only $\sim 1\%$ of the interactions produce charm. Hadronic interactions, on the other hand, produce charm in a ratio of $1 : 10^3$ only and are therefore not useful for charm lifetime measurement with the emulsion technique.

Two of the emulsion experiments accumulated relatively high statistics and are therefore discussed in this report.

A) Experiment WA 58 [9]

To produce the charmed particles a tagged photon beam with an energy between 20 and 70 GeV was sent to an emulsion target. The Omega spectrometer in CERN was used as downstream spectrometer to find and to reconstruct the charm events.

The experimental set-up is given in fig. 6. The spectrometer consisted of a large magnet, of a series of proportional chambers (MWPC and WPC) to detect and analyse the charged particles, and of further detectors for particle identification. As emulsion vertex detector 6000 emulsion pellicles of the dimension of 20 cm x 5 cm x 600 μm (36 l) were used. A mechanical device brought single pellicles, one at a time, to the target position where they were put at an angle of 5° to the beam axis, so that their effective thickness was about 6 mm. Each pellicle was irradiated by 10^6 tagged photons.

The outgoing particle tracks as recorded in the spectrometer served to predict the interaction region in the emulsion to be scanned subsequently.

A typical example of an interaction in the emulsion is seen in fig. 7, which shows the decays of a Λ_c and of a D^0 . At the point O' the Λ_c decays into $\Lambda^0 \pi^+$. The track 4.1 corresponds to the π^+ -meson. The Λ itself does not decay in the emulsion, but downstream in the spectrometer; the corresponding tracks of p and π^- are labeled by the numbers 7 and 8. The second charmed decay is at the point O'', where D^0 decays into $\pi^- K^+ \pi^+ \pi^+$. The lifetimes of the two particles were determined to $t_{\Lambda_c} = (0.5 \pm 0.02) \cdot 10^{-13}$ sec and $t_{D^0} = (0.86 \pm 0.01) \cdot 10^{-13}$ sec.

Up to now, from 160 K triggers recorded in the spectrometer 45 K triggers (~30%) were scanned, giving a sample of 22 D^0 events and 7 Λ_c events for lifetime measurement. Most of the D^0 's decayed in the Cabibbo-allowed decay channels $K^+ \pi^- (\pi^+ \pi^- n \pi^0 \text{'s})$ or $K^0 \pi^+ \pi^- (\pi^+ \pi^- n \pi^0 \text{'s})$. Other decay modes as the semileptonic decay $K^0 \pi^- e^+ (\nu)$ or $K^+ \pi^0 \pi^0 e^- (\bar{\nu})$ and the exotic twice Cabibbo suppressed decay $D^0 \rightarrow K^- \pi^+ \pi^0$ (K^- and π^+ identified) were also observed. The Λ_c decays into $\Lambda^0 \pi^+ (\pi^0)$ and $p \bar{K}^0 (\pi^0)$ were seen. The results of the lifetime determination as reported at the Brighton Conference are:

$$22 D^0: \quad \tau_{D^0} = (2.3 \begin{smallmatrix} +1.4 \\ -0.7 \end{smallmatrix} \pm 0.7) \cdot 10^{-13} \text{ sec}$$

$$7 \Lambda_c: \quad \tau_{\Lambda_c} = (2.1 \begin{smallmatrix} +1.1 \\ -0.7 \end{smallmatrix} \pm 0.5) \cdot 10^{-13} \text{ sec.}$$

The first error values correspond to statistical errors and the second one takes the systematic uncertainties into account.

- 9 -

B) Experiment E 531 | 10 |

This emulsion experiment, carried out in Fermi Lab, used a single-horn focused neutrino beam. Secondary charged particles from the interactions in the emulsion target are traced in the downstream spectrometer, consisting of a magnet and of drift chambers DCI and DCII (see schematic layout of the experiment in fig. 8). For particle identification time of flight is measured with an accuracy of ~ 120 psec by a thirty-element scintillator hodoscope. This is followed by a wall of sixty-eight $19 \text{ cm} \times 19 \text{ cm} \times 30 \text{ cm}$ lead-glass blocks for electron and photon registration. A simple hadron calorimeter contains five layers of iron each 10 cm thick interleaved with planes of four vertical scintillators each 2.4 m high by 0.75 m wide. This is followed by a muon filter with scintillator hodoscopes behind 1.2 and 2.9 m iron.

The emulsion target consists of 12 modules, each containing 177 emulsion pellicles $14 \text{ cm} \times 5 \text{ cm} \times 600 \mu\text{m}$ parallel to the beam and of 27 modules of 68 films of polystyrene $12 \text{ cm} \times 9.5 \text{ cm}$, $70 \mu\text{m}$ thick and coated on both sides with $330 \mu\text{m}$ of emulsion. The planes of the latter films were perpendicular to the beam. A fiducial sheet of lucite, coated in both sides with emulsion covered all the emulsion stacks and was located relative to them to a precision of better than $100 \mu\text{m}$ by marks irradiated by a collimated x-ray source. It served to relate individual tracks from the drift chambers to the emulsion target.

Reconstructed event tracks in the spectrometer predicted the vertex in the emulsion target, which was searched for either by a volume scan or by track following into the emulsion.

The results of the experiment came from 2 runs with 24 l and 32 l of emulsion resp. This gave ~ 1800 and ~ 3800 spectrometer predictions in the emulsion target. As reported at the Paris Conference 1982, the following results refer to the first run only.

The charged decay search located 23 multiprong decays and 5 single prong kinks as good candidates for charm decay. A search for neutral decays yielded 21 neutral charm candidates. Identification of the decaying charmed particles was accomplished by kinematic fitting and by means of particle identification in the spectrometer and the emulsion. This resulted in 19 D^0 , 11 D^+ , 3 F^+ and 8 Λ_c . Part of the D^+ are ambiguous with F^+ or Λ_c . On the other hand, the F^+ and Λ_c samples are claimed to be clean.

Table 6

decay channel	decay length (μm)	momentum (GeV/c)	decay time (10^{-13} sec)
$F^+ \rightarrow \underline{K^+} \underline{\pi^+} \underline{\pi^0} \underline{K^-}$	130	9.33	0.94
$+ \underline{K^+} \underline{K^+} \underline{\pi^+} \underline{\pi^0}$	132	5.93	1.51
$F^- \rightarrow \underline{\pi^+} \underline{\pi^+} \underline{\pi^0} \underline{\pi^-}$	670	12.25	3.90
$\Lambda_c^+ \rightarrow \underline{\Lambda^0} \underline{\pi^+} \underline{\pi^+} \underline{\pi^-}$	41	5.73	0.54
$+ \underline{\Lambda^0} \underline{\pi^+} \underline{\pi^+} \underline{\pi^-}$	180	8.40	1.63
$+ \underline{\Lambda^0} \underline{\pi^+} \underline{\pi^+} \underline{\pi^-}$	221	4.67	3.60
$\rightarrow \underline{p} \underline{K_L^0}$	175	5.80	2.30
$\rightarrow \underline{p} \underline{\pi^+} \underline{K^-} (\underline{\pi^0})$	21	1.9 <u>or</u> 2.7	0.60 <u>or</u> 0.40
$\rightarrow \underline{p} \underline{\pi^+} \underline{\pi^-} (\underline{K^0})$	28	2.9 <u>or</u> 5.0	0.73 <u>or</u> 0.42

In Table 6 the F^\pm and Λ_c candidates are listed together with their decay lengths, momenta of the charmed particle and with the decay time. Particles are underlined if they were identified in the spectrometer. The particles in parenthesis were added in order to balance the transverse momentum of the corresponding charm decay. The protons of the Λ -decays were always identified in the spectrometer. The mean lifetimes of these charmed particles were determined with the maximum likelihood method and the results are:

$$3 F^\pm: \tau = (2.0 \begin{smallmatrix} + 1.8 \\ - 0.8 \end{smallmatrix}) \cdot 10^{-13} \text{ sec}$$

$$8 \Lambda_c: \tau = (2.3 \begin{smallmatrix} + 1.0 \\ - 0.6 \end{smallmatrix}) \cdot 10^{-13} \text{ sec}$$

$$11 D^\pm: \tau = (11.4 \begin{smallmatrix} + 6.6 \\ - 4.4 \end{smallmatrix}) \cdot 10^{-13} \text{ sec}$$

$$19 D^0: \tau = (3.2 \begin{smallmatrix} + 1.0 \\ - 0.7 \end{smallmatrix}) \cdot 10^{-13} \text{ sec.}$$

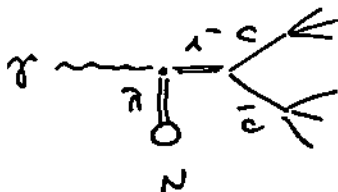
4. ELECTRONIC EXPERIMENTS

Charmed particle lifetimes have been measured by several electronic experiments. Here the interaction and the charm decay are not detected by visual inspection of the reaction as in emulsion or bubble chamber experiments, but by electronic devices. There are essentially two methods used for this purpose. In the first, the increase of charged multiplicity due to charm decay, downstream of the interaction, is measured in a so called living target (NA 1). In the second method, the interaction and decay vertices are reconstructed by extrapolation of tracks measured in either precise drift chambers (MARK II) or in microstrip silicon detectors (ACCOMR).

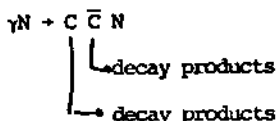
-11-

A) Experiment NA 1 [14]

In this experiment the coherent photoproduction on nuclei is used to produce a pair of charmed particles whose decays are investigated.



The corresponding reaction is



The experimental layout of this CERN experiment is schematically seen in fig. 9. It consists of the beam set-up, the living target and a downstream spectrometer. The single elements are described as follows.

An electron beam is sent to a lead converter with a thickness of 0.1 radiation length. The produced bremsstrahlung-photons of energies ranging from 40 to 150 GeV reach the target as shown in fig. 9. The scattered electrons are tagged in a hodoscope providing the photon energy with an accuracy of $\pm 5\%$.

The target consists of 40 silicon semiconductor counters, 300 μm thick, separated by gaps of 100 μm . Each counter gives a signal corresponding to the ionisation of the throughgoing particle.

Therefore, using the pulse-height pattern of the silicon detectors the number of passing charged particles can be determined in each layer. The layer in which the interaction occurs is found by the high signal produced by the recoiling nucleus. Low pulse heights are observed in the subsequent set of layers by the two charged charm particles. A higher pulse height is found in the layers downstream of the charm decay when the multiplicity increases by at least two units. Fig. 10 shows the pulse height pattern for an event when a pair of charm particles is produced and subsequently decays.

The target is surrounded by a set of veto counters for charged particles and photons in order to eliminate incoherent multiparticle events. The forward spectrometer consists of 4 magnets to bend charged particles into the drift chambers in such a way that more energetic particles cross more magnetic fields, giving a roughly uniform momentum resolution between 1 and 150 GeV/c. In front

of each magnet shower detectors (sandwiches of lead and scintillator hodoscopes) detect photons from π^0 -decays. Inside magnet 1 and 2, two multicell Cerenkov counters separate pions from kaons in the momentum range 5 to 21 GeV/c.

The target does not tell us how the particles detected in the spectrometer should be associated to the two charm decays. Therefore the particles are separated into two groups and the effective masses are calculated. A combination of particles is accepted if each group has the expected mass value (mass of a charmed particle) and contains the particles expected for the corresponding charm decay. All events in the target are further examined and only those are retained which show a step structure in the pulse height of the silicon layers (a step being identified if it extends at least over 4 silicon strips).

For D^{\pm} lifetime measurement a sample of 74 events with a single step and 12 events with two steps (therefore 24 decays) are used. The F^{\pm} as observed in this experiment decays into $\eta \pi^+ \pi^- \pi^0$ and $K^+ K^- \pi^+ \pi^0$. The corresponding distributions are, however, not very convincing. This could be due to lack of statistics. For F^{\pm} lifetime determination, 8 events were used which showed the expected step structure in the silicon layers. For each decay the flight length between production and decay of the charmed particles was measured and the lifetime was determined by a maximum likelihood fit. The results are:

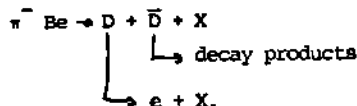
$$98 D^{\pm}: \tau = (9.5 \pm 3.1 \text{ } ^{-1.9}) \cdot 10^{-13} \text{ sec}$$

$$8 F^{\pm}: \tau = (5 \pm 5 \text{ } ^{-2.5}) \cdot 10^{-13} \text{ sec.}$$

B) ACCMOR-Collaboration [15]

This experiment carried out at CERN uses the NA 11-spectrometer together with a telescope of silicon microstrip detectors (MSD). Its schematic layout is shown in fig. 11.

An unseparated π^- beam at 200 GeV/c was sent to a Be target, in which charmed D-mesons were produced and selected by an electron trigger.



The forward produced hadronic system was measured in the downstream spectrometer, consisting of two magnets (M1, M2) and 48 planes of large drift chambers arranged in four packs (ARM2, 3a, 3b, 3c). Three multicell Cerenkov counters (C1, C2, C3) allowed identification of $\pi/K/p$ in the momentum range from 4 to 8 GeV/c, and a photon calorimeter (γ -CAL) detected the photons. The trigger system is explained in fig. 12. Using the multicell Cerenkov counter Q and the lead scintillator calorimeter (E-CAL) electron events are selected.

-13-

For the offline reconstruction of the events, 6 MSD's were used to measure with great precision ($\sigma_{hor} = 25 \mu\text{m}$, $\sigma_{vert} = 6 \mu\text{m}$) the position of the incident beam to the Be-target and 6 MSD's measured the charged particles produced in the reaction with a spatial resolution of $4.5 \mu\text{m}$ (this refers to the central region of MSD). The typical accuracy of the reconstruction of the position of the primary vertex along the beam direction was $150 \mu\text{m}$.

The results are obtained from the analysis of $4.4 \cdot 10^4$ triggers. After offline selection of events with an electron and a charged kaon and after rejection of electron pairs $1,5 \cdot 10^3$ events remained, for which the analysis using the MSD information was done. The tracks found in the drift chambers are connected with the tracks found in the MSD and the interaction vertex in the Be target as well as a secondary decay vertex are reconstructed (see fig. 13).

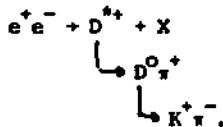
After applying various cuts 23 fully reconstructed D^0 decaying into $K^+ \pi^-$ or $K^+ \pi^+ \pi^-$ and 13 D^+ decaying into $K^+ \pi^+ \pi^+$ are used to calculate the lifetime. The results are:

$$\begin{aligned} 23 D^0 \quad \tau &= (4.2 \pm 1.0) \cdot 10^{-13} \text{ sec} \\ 13 D^+ \quad \tau &= (8.8 \pm 2.7) \cdot 10^{-13} \text{ sec.} \end{aligned}$$

C) MARKII-Collaboration [16]

Preliminary results of a lifetime determination of the D^0 in the MARK II-detector (see fig. 14) at PEP (SLAC) were presented at the Paris Conference 1982. The technique used was almost identical to that used by the same collaboration for the determination of the lifetime of the τ -lepton [17]. The new MARK II vertex detector surrounding the beam pipe provides good position measurements of the tracks (4 position measurements at a radius of ~ 12 cm and 3 position measurements at a radius of ~ 30 cm).

At an energy of $E_{CM} = 29$ GeV, 7 D^0 -decays were identified in the reaction



Fitting the tracks of the D^0 -decay products, the D^0 -decay vertex was found with a precision of $700 \mu\text{m}$. The flight length of the D^0 was determined by measuring the distance between the decay vertex and the $e^+ e^-$ interaction point. Typical flight lengths are $\sim 500 \mu\text{m}$. Since the mean flight distance is in the same order as the experimental resolution, the lifetime can only be determined by statistical averaging. The result is

$$7 D^0 \quad \tau = (3.7 \pm 2.5 - 1.5) \pm 1.0) \cdot 10^{-13} \text{ sec.}$$

5. CONCLUSION

In a serie of experiments the lifetimes of the charmed particles D^+ , D^0 , F^+ and Λ_c have been determined. The results of these measurements as well as the mean value are displayed in fig. 15. The mean values are [18]:

$$D^+: \tau = (8.8 \pm 1.3 \text{ } -1.0) \cdot 10^{-12} \text{ sec}$$

$$D^0: \tau = (4.4 \pm 0.6 \text{ } -0.5) \cdot 10^{-12} \text{ sec}$$

$$F^+: \tau = (2.1 \pm 1.3 \text{ } -0.6) \cdot 10^{-12} \text{ sec}$$

$$\Lambda_c: \tau = (2.2 \pm 0.8 \text{ } -0.5) \cdot 10^{-12} \text{ sec.}$$

Since the values differ from particle to particle, it can be concluded that the spectator model alone cannot explain the decay. Other graphs (see fig. 2) seem also to be important.

The ratio $\tau_{D^+}/\tau_{D^0} = 2.0 \pm 0.4$ is related to the semileptonic branching ratios of D^+ and D^0 (B_{D^+} and B_{D^0} resp.) if only Cabibbo allowed decays are taken into account [19]. It is

$$\tau_{D^+}/\tau_{D^0} = B_{D^+}/B_{D^0}$$

The ratio $B_{D^+} = (19 \pm 4 \text{ } -3) \%$ $B_{D^0} < 6\%$ is somewhat too high to be in agreement with the above prediction [20].

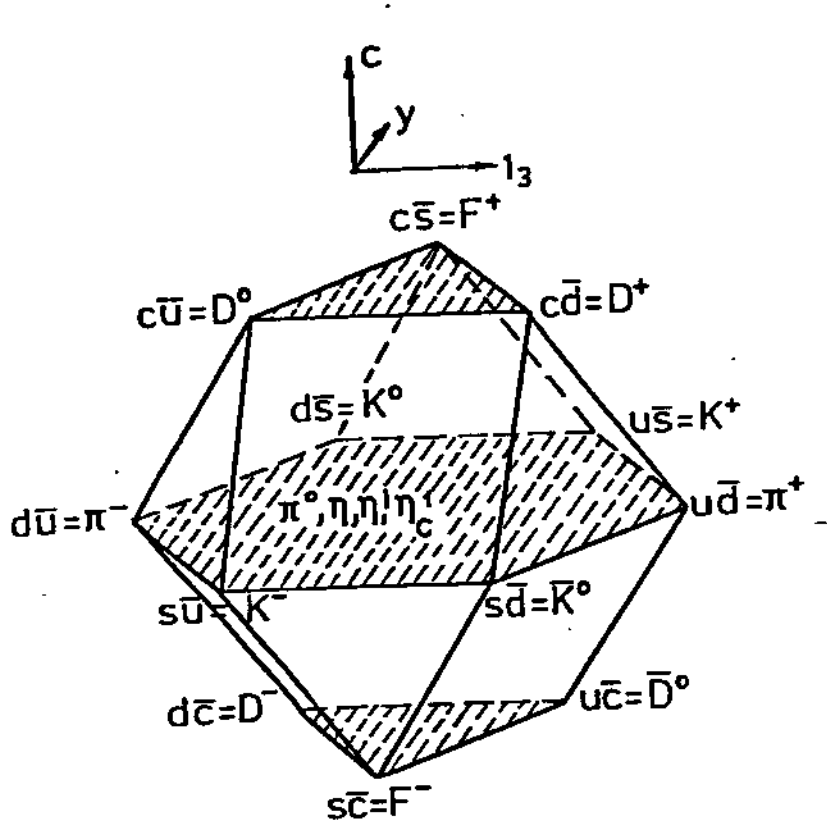
REFERENCES

- [1] J. Sandweiss, Phys. Rep. 83 (1982) 39
 G. Bellini, L. Foa, M.A. Giorgi, Phys. Rep. 83 (1982) 9
 J.D. Prentice, Phys. Re. 83 (1982) 85
 L. Montanet, S. Reucroft, Phys. Rep. 83 (1982) 61
- [2] G.H. Trilling, Phys. Rep. 75 (1981) 57
 G. Goldhaber, J.E. Wiss, Ann. Rev. Nucl. Part. Sci. 30 (1980) 337
 M.K. Gaillard, B.W. Lee, J.L. Rosner, Rev. Mod. Phys. 47 (1975) 277
 F. Muller, CERN-EP/83-67 (18 Aug. 1983)
- [3] J.J. Aubert et al., Phys. Rev. Lett. 33 (1974) 1404
 J.E. Augustin et al., Phys. Rev. Lett. 33 (1974) 1406
- [4] G. Kalmus, Weak decays of new particles, Rapp. Talk at the International Conference on High Energy Physics, 1982, Paris
- [5] A. Chen et al., Phys. Rev. Lett. 51 (1983) 634
- [6] S.F. Biagi et al., Phys. Lett. 122B (1983) 455
- [7] L.S. Glashow, J. Iliopoulos, L. Maiani, Phys. Rev. D2 (1970) 1285
- [8] M. Kobayashi, T. Maskawa, Prog. Theor. Phys. 49 (1973) 652
 L.L. Chan, Phys. Rep. 95 (1983) 1
- [9] M.D. Adamovich et al., Phys. Lett. 99B (1981) 271
 A. Fiorino et al., Lett. Nuovo Cim. 30 (1981) 166
 Contributions to the International Conferences on High Energy Physics at Paris (1982) and Brighton (1983)
- [10] N. Ushida et al., Phys. Rev. Lett. 45 (1980) 1049
 N. Ushida et al., Phys. Rev. Lett. 45 (1980) 1053
 N. Ushida et al., Phys. Rev. Lett. 48 (1982) 844
- [11] Contribution to the International Conference on High Energy Physics, Paris (1982)
 M. Aguilar-Benitez et al., Phys. Lett. 122B (1983) 312
- [12] K. Abe et al., Phys. Rev. Lett. 48 (1982) 1526
 Contributions to the International Conferences on High Energy Physics at Paris (1982) and Brighton (1983)
- [13] Contribution to the International Conference on High Energy Physics at Paris (1982)
 Badertscher et al., Phys. Lett. 123B (1983) 471
- [14] S.R. Amendolia et al., Nucl. Instr. and Meth. 176 (1980) 449
 G. Bellini et al., Nucl. Instr. and Meth. 196 (1982) 351
 E. Albini et al., Phys. Lett. 110B (1982) 339
 Contribution to the International Conference on High Energy Physics, Paris (1982)
- [15] Contributions to the International Conference on High Energy Physics at Brighton (1983): R. Bailey et al., (A Vertex telescope of 5 μ m resolution silicon strip detectors for the observation of charm events) and P. Bailey et al. (A lifetime measurement of hadronically produced D mesons)
 B. Hyams et al., Nucl. Instr. and Meth. 205 (1983) 99

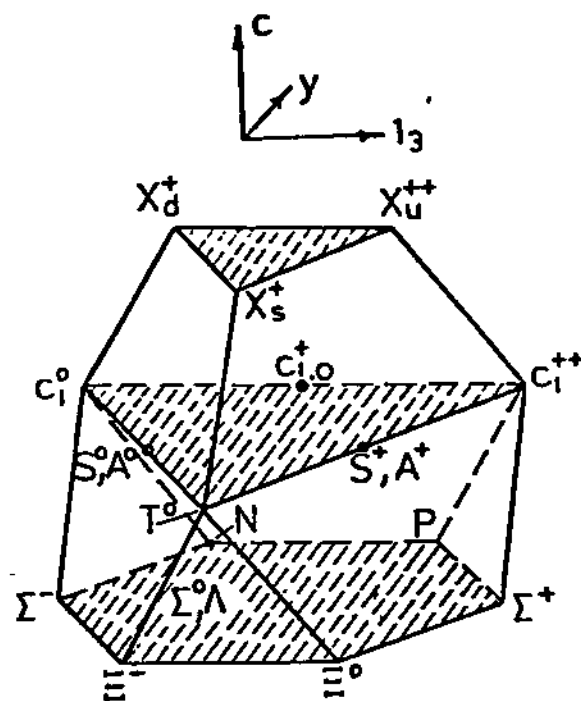
- [16] Contribution to the International Conference on High Energy Physics at Paris (1982)
- [17] G.J. Feldman et al., Phys. Rev. Lett. 48 (1982) 66
- [18] C. Jarlskog, Weak decays, Rapp. Talk at the International Conference on High Energy Physics, 1983, Brighton
- [19] A. Pais, S. B. Treiman, Phys. Rev. D15 (1977) 2529
- [20] M. Roos et al., Phys, Lett. 111B (1982) 1

SU(4) - predictions

Fig.1



0^- - mesons

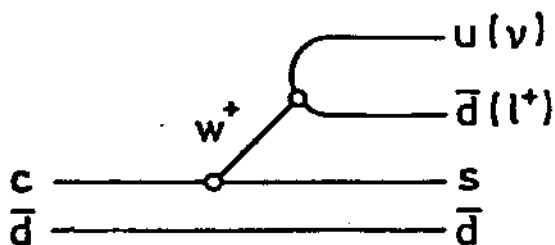


$1/2^+$ - baryons

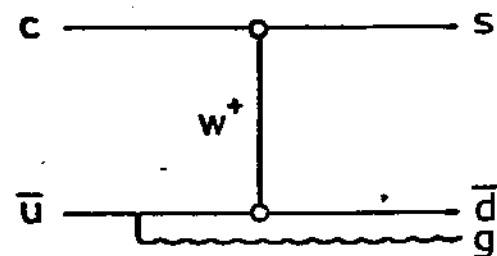
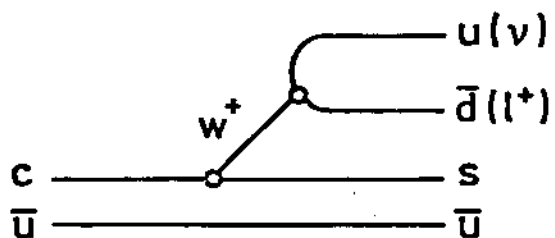
Decay diagrams
Cabibbo-allowed

Fig.2

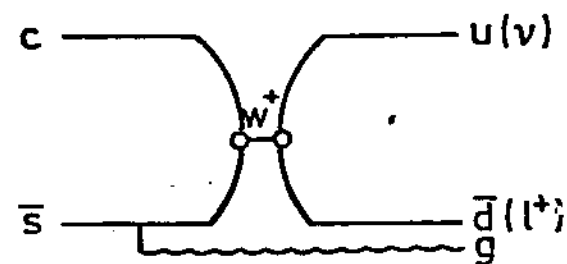
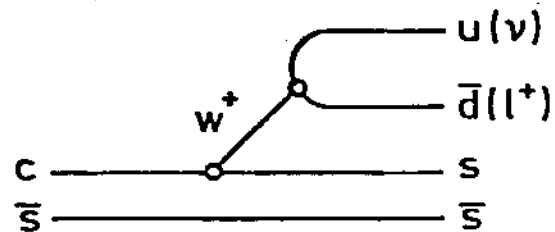
D^+



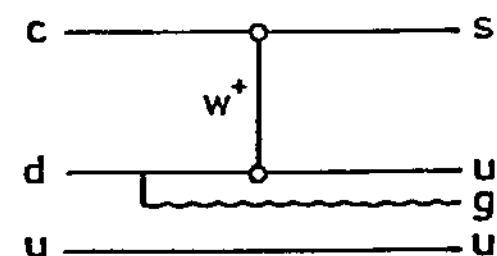
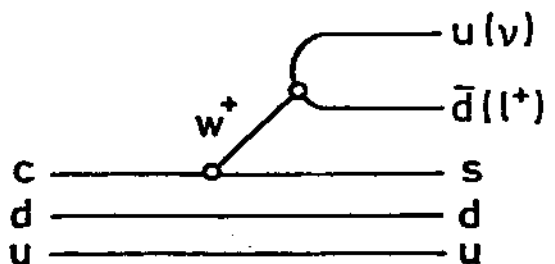
D^0



F^+

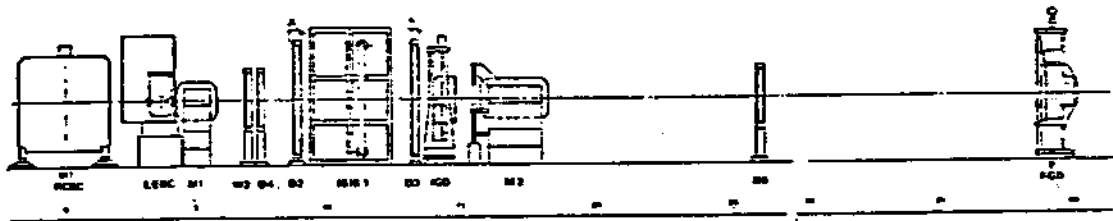


Λ_c



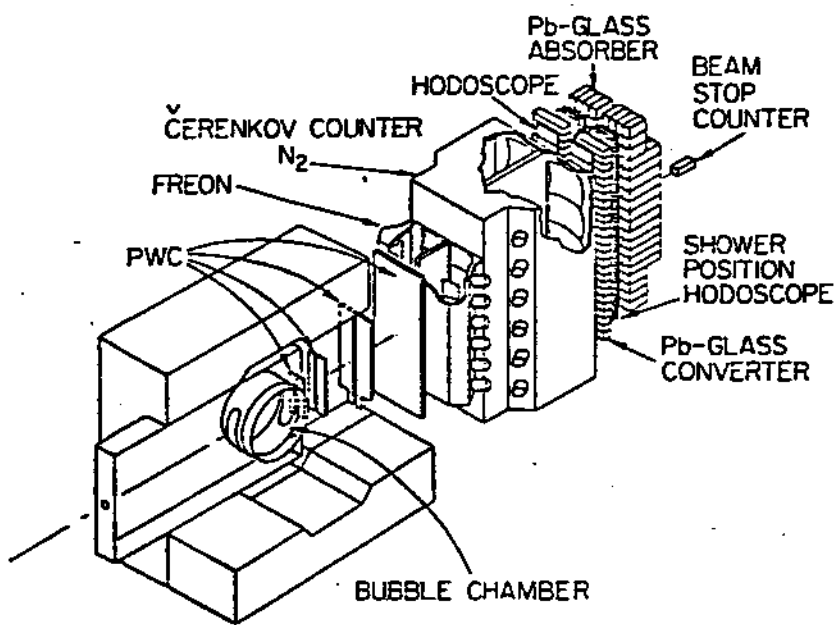
NA 16 set - up

Fig.3



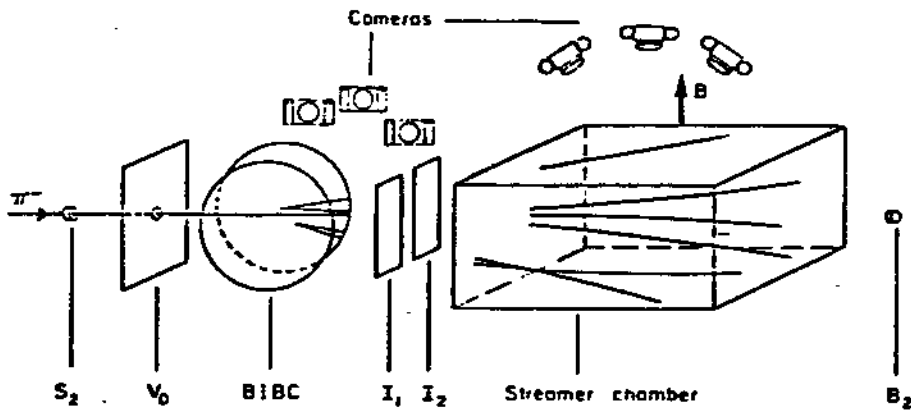
BC 73 set - up

Fig.4



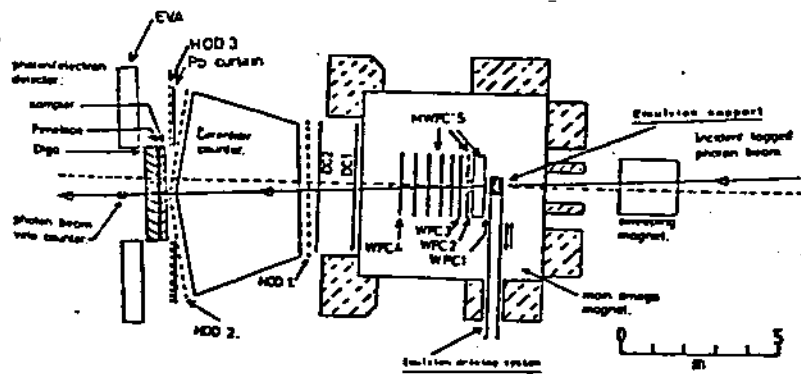
NA 18 set - up

Fig.5



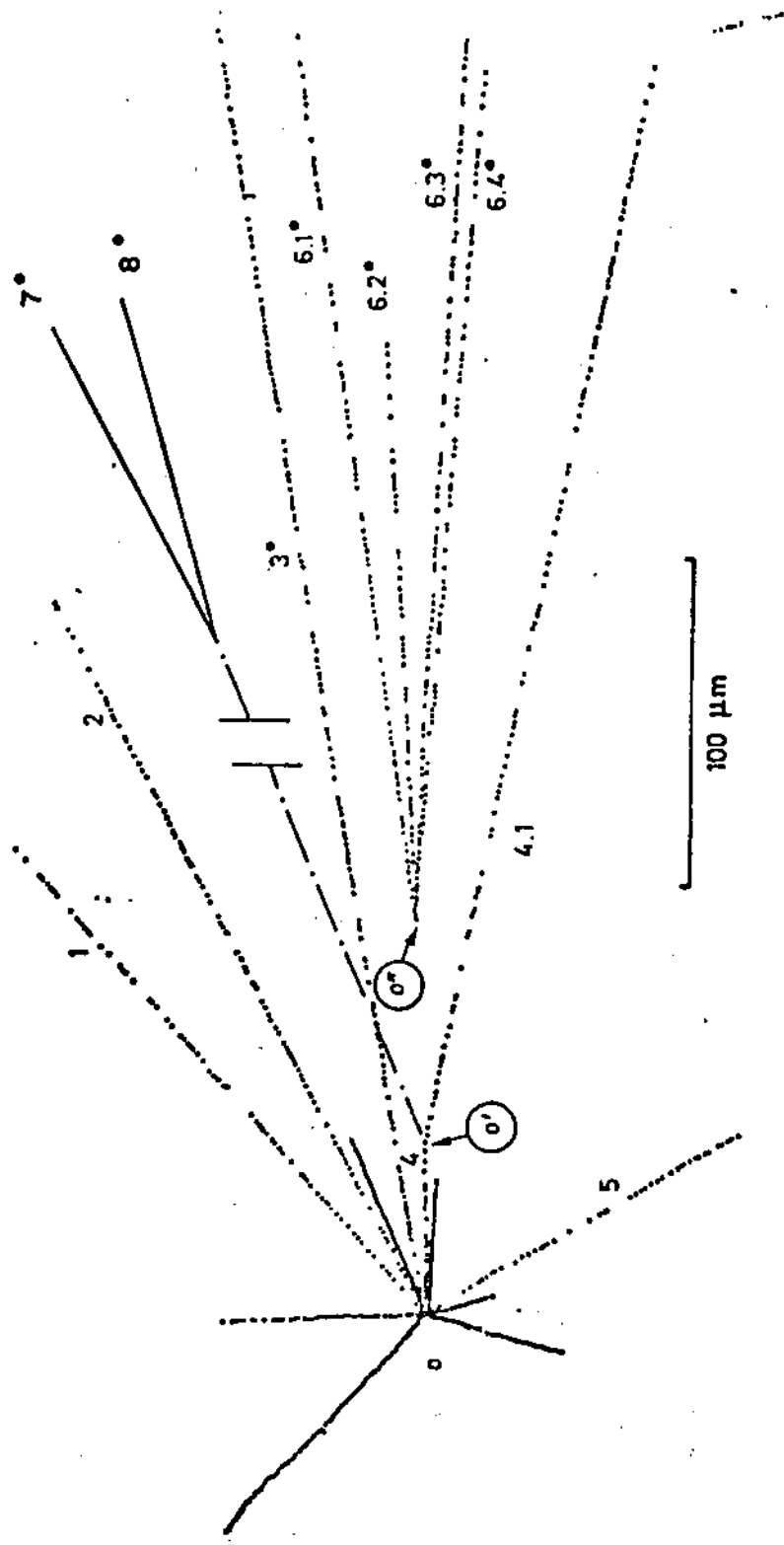
WA 58 set-up

Fig.6



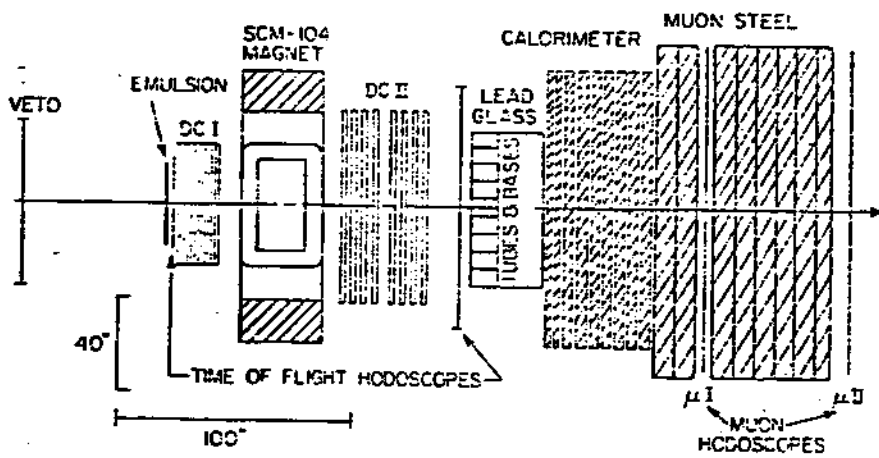
Interaction in the emulsion

Fig. 7



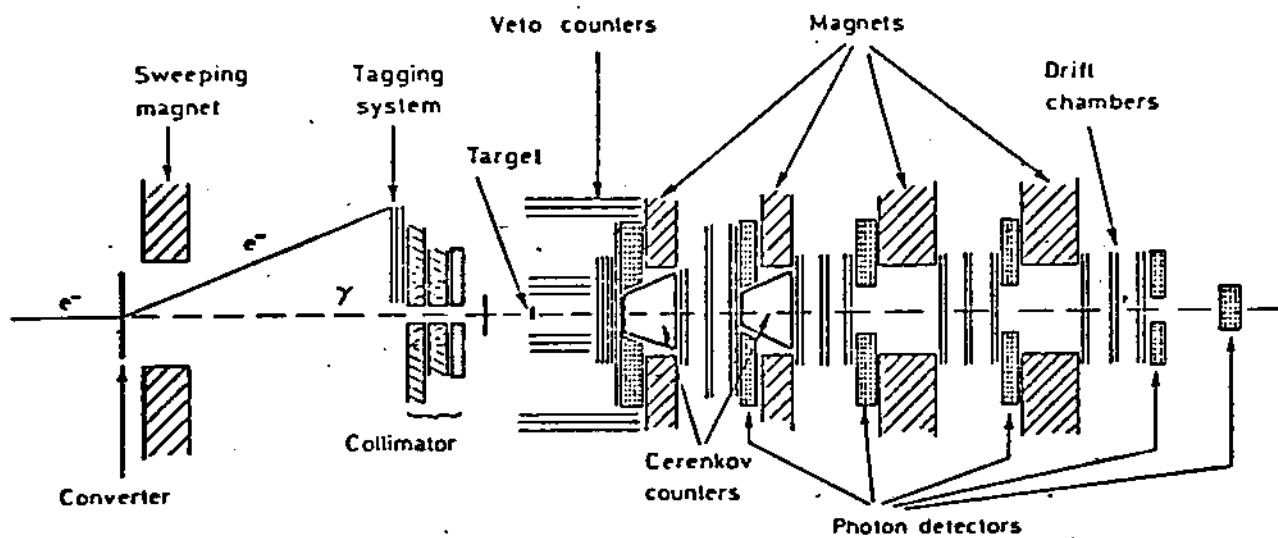
E 531 set-up

Fig.8



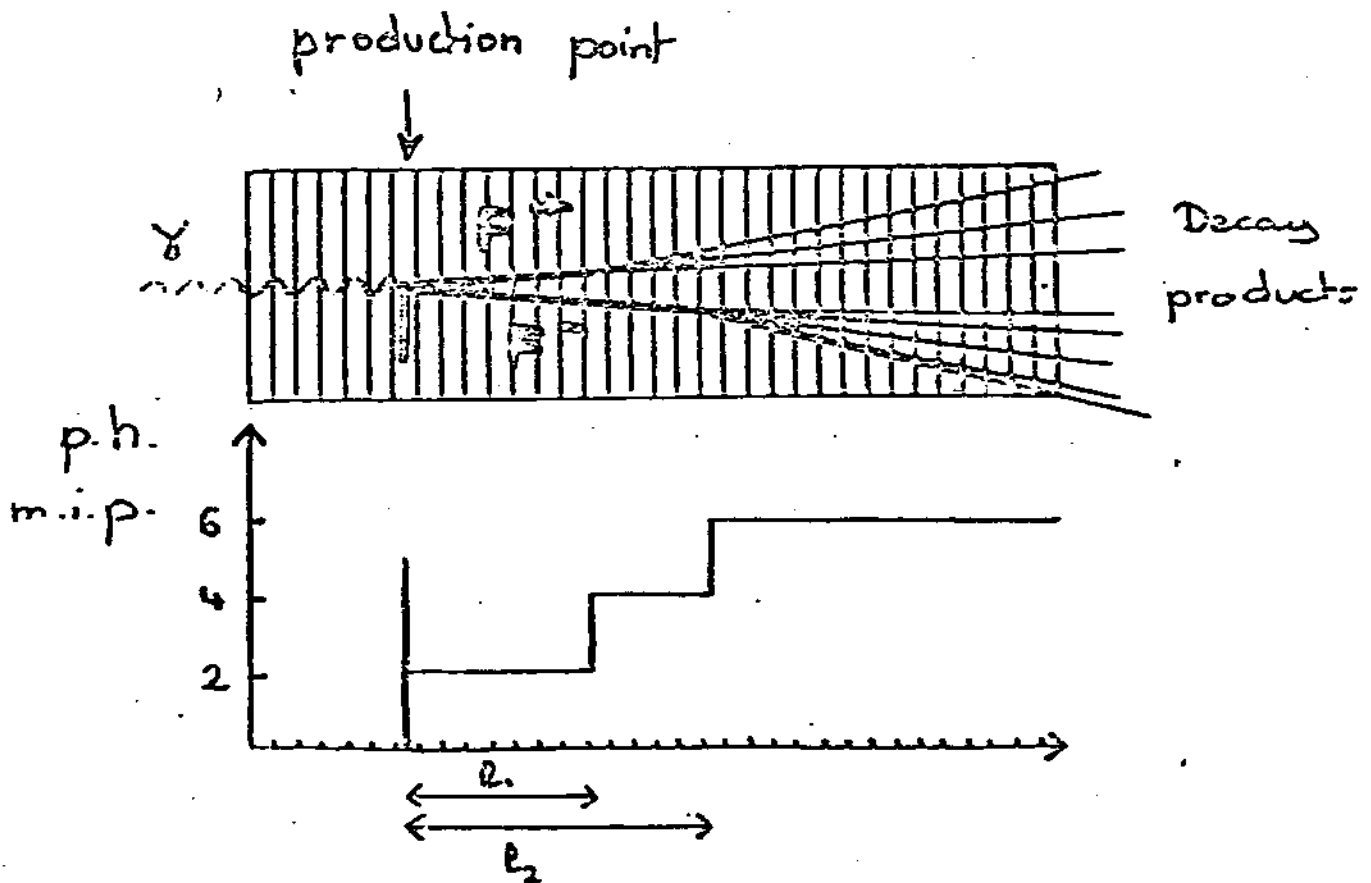
NA 1 set-up

Fig.9



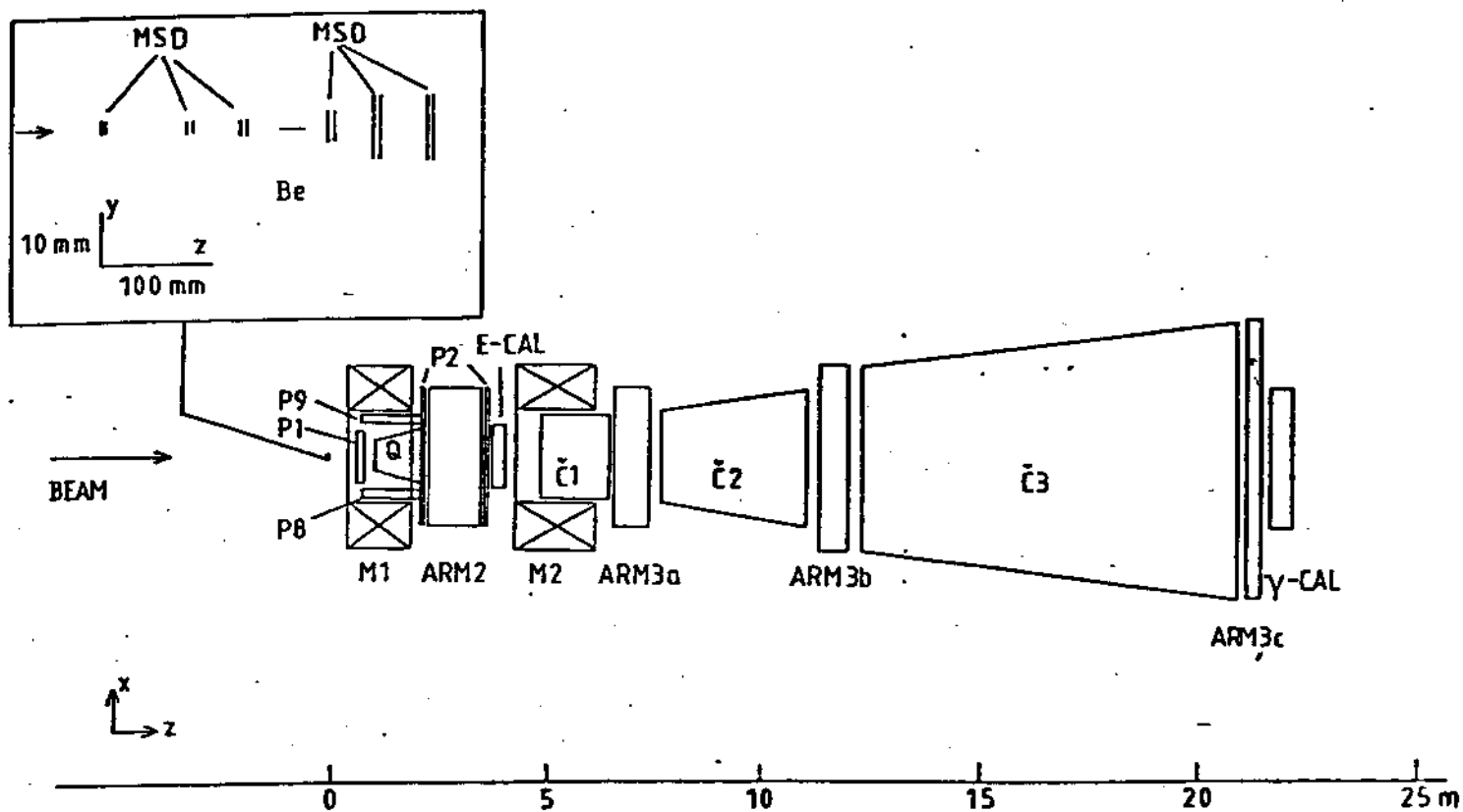
Pulse height for γ Si \rightarrow Si F⁺ F⁻

Fig.10

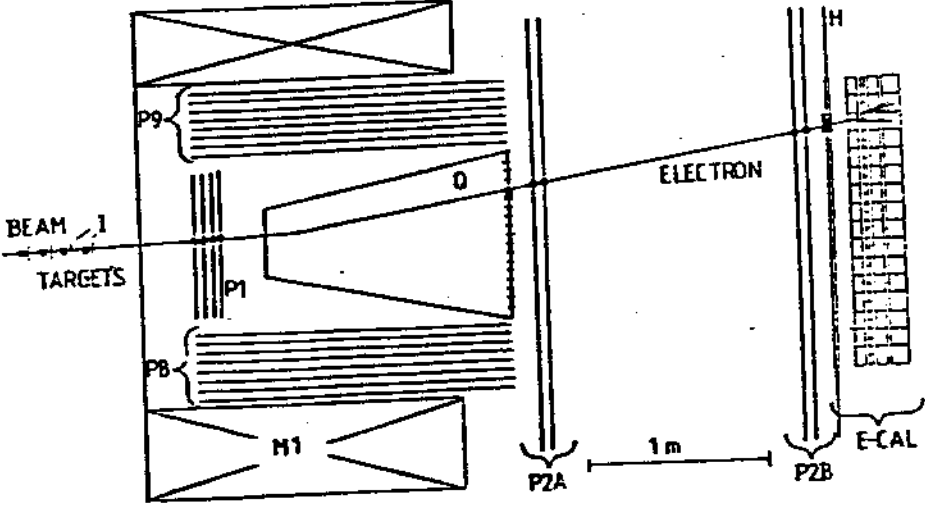


Set-up of ACCMOR - collaboration

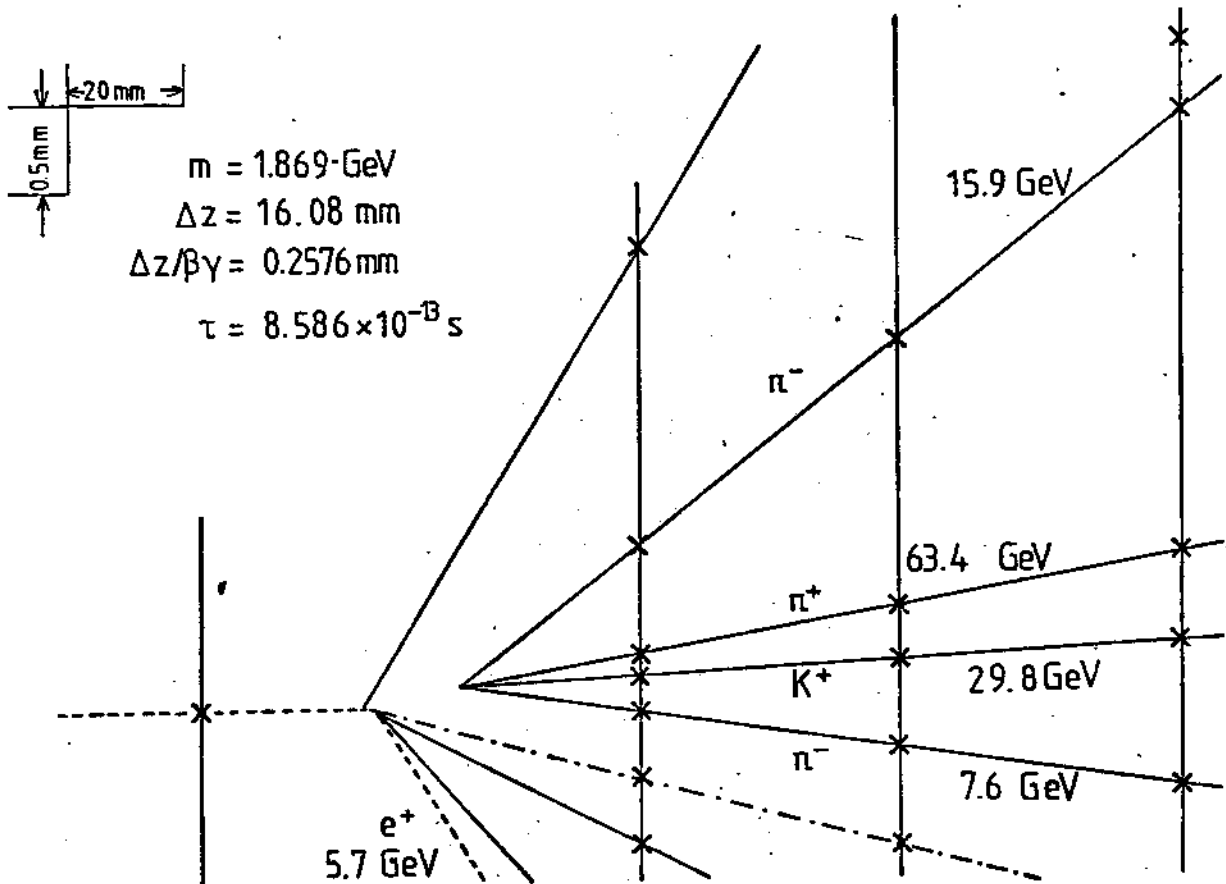
Fig.11



Trigger system of ACCMOR-collaboration Fig.12

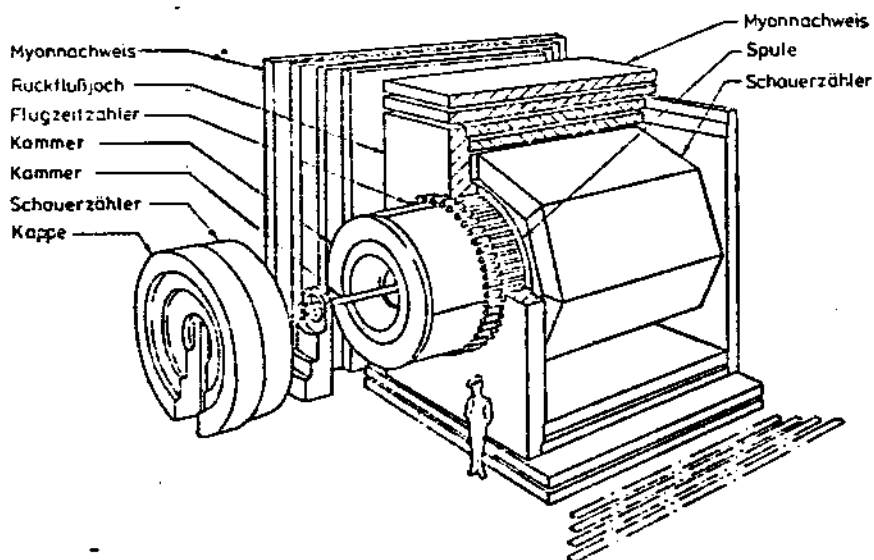


Reconstructed tracks from MSD information Fig.13



MARK II set - up

Fig.14



D⁰ and D[±] lifetimes

Fig.15

